Morpho-Physiological Traces of Exogenous Biogenic Iron Oxide Nanoparticles in Basil Seedlings

Semra Kilic,[a,*] Sercan Onder,[b] Damla Onder,[a] Havva Kaya,[c] and Aziz Sencan [d]

Chemical fertilizers used in plant development and differentiation have become a global problem affecting the entire ecosystem, especially soil pollution. Food production demand with the increasing population has encouraged scientists to use biogenic nanoparticles in the agricultural field. Evaluation of growth, development, and differentiation processes of sweet basil (*Ocimum basilicum* L.) seedlings at gradually increasing concentrations of biogenic iron oxide nanoparticles (BIO-NPs) were identified by morphological and physiological parameters in this study. The results showed that growth parameters reached the maximum value at 100 mg/L but were less at other concentrations. At similar concentration, the stomatal density of the leaf was the maximum, while the stomatal area showed the lowest value. The levels of H_2O_2 and malondialdehyde (MDA) decreased in the treated seedlings. BIO-NPs increased the antioxidant defense and supported its growth by changing the antioxidant enzyme activities, H_2O_2, and MDA contents. The BIO-NP treatment provided positive improvements in phytochemical content in parallel with the growth and development of sweet basil seedlings. Different growth parameters, physiological results, supporting enzyme activities, and biochemical data revealed the contribution of the BIO-NP treatments to the growth and development of sweet basil seedlings. BIO-NPs improved higher phytochemical production of sweet basil, which may be suitable for its propagation on a commercial scale.

DOI: 10.15376/biores.19.3.4434-4454

Keywords: Antioxidative enzymes; Glandular trichomes; Hydrogen peroxide; Ocimum basilicum; Phytochemicals

*Contact information: a: Department of Biology, Suleyman Demirel University, 32260, Isparta/Turkey; b: Isparta University of Applied Sciences, Faculty of Agriculture, Department of Agricultural Biotechnology, Isparta, Turkey; c: Department of Bioengineering, Suleyman Demirel University, 32260, Isparta/ Turkey; d: Department of Chemical Engineering, Suleyman Demirel University, 32260, Isparta/ Turkey; *Corresponding author: semrakilic@sdu.edu.tr*

INTRODUCTION

Nanoparticles (NPs) have shown very good catalytic, magnetic, electrical, mechanical, optical, chemical, and biological abilities because of their high surface area and high reactivity, and the desired level of tunability of the particle size. Therefore, its use in many areas of industries, especially in agriculture, is considered an appropriate strategy. Because physical and chemical methods of nanoparticle production require toxic chemicals and high energy consumption, they cause both environmental pollution and high costs, and it has been concluded that the use of biological methods in nanoparticle synthesis is more effective (Zawadzka *et al.* 2021). When the quantity of nano-sized particles increases, their surface width increases and more molecules on the surface are exposed (Macera *et al*.

2020). This enables them to bind more molecules, thus significantly accelerating their catalytic properties.

Plants require many micro- and macro-nutrients that are vital for optimum growth, development, and productivity of plants. Although iron, which is the essential micronutrient for plants, is required in small amounts, it is a co-factor for catalyst enzymes in the initiation and maintenance of various biochemical reactions, especially in RNA synthesis and in the Calvin cycle (Morales *et al*. 2020). Iron plays an important role in many physiological activities such as photosynthesis, chloroplast development, enzymatic activity of respiration, rubisco activity, and closure of stomata (Alkhatib *et al*. 2019). Although iron is found in high amounts in the soil (Fe^{3+}), the bioavailability of the plant is adversely affected because its solubility is quite low (Zhang *et al*. 2022). Fe is found in the soil in the form of insoluble Ferric oxide (Fe^{3+}). Ferrous ion (Fe^{2+}), formed by microbial reduction in anaerobic conditions in the presence of excess water, is easily absorbed by plants and stored in the leaves, causing toxicity (Nozoe *et al*. 2009). Although Fe is a necessary micronutrient for the plant life cycle, its excessive amount in the environment causes a series of physiological deteriorations that lead to the death of the plant. In particular, rapid cell death occurs by disrupting the respiratory and photosynthetic activity of the plant, enzymatic activity processes, and causing the degradation of important biomolecules. (Zahra *et al*. 2021). Iron nanoparticles (Fe-NPs) are very small and have a high capacity to bind to different molecules, their strong absorbing properties and potential to be easily separated from the environment facilitate their gradual uptake by the plant, and these properties enable it to readily participate in various biochemical reactions (Poddar *et al*. 2020). A significant amount of iron is localized in the chloroplasts of plants. Therefore, it is not surprising that iron deficiency in higher plants leads to changes in the structure and function of the entire photosynthetic system, which in turn results in disturbances in lipid composition and a change in chlorophyll content (Feng *et al*. 2022). Generally, significant reductions in root length, shoot length, biomass, and chlorophyll contents were observed in plants with concomitant increase in lipid peroxidation, ROS production, and H_2O_2 contents. Therefore, nanoparticles are an important approach for the gradual release of the elements needed by the plant, and with the high reactivity and catalyst role of nanoparticles, intracellular chemical changes occur simplify. Due to the extraordinarily small dimensions, large surface areas, and high stability of Fe-NPs, it can show quite a lot of activity even at low concentration, as the solubility of iron increases (Ranjan *et al*. 2022). Although it is known that BIO-NPs significantly affect the secondary metabolite contents of plants (Kruszka *et al*. 2022), the morpho-physiological changes that occur in this process are not known. In fact, no data were found regarding physiological parameters that are coordinated with the growth and development of sweet basil seedlings of BIO-NPs. This study aimed to determine the optimal concentrations of BIO-NPs required for the growth and development of sweet basil seedlings, as well as identification of their phytochemical content and antioxidant enzyme activity, and to determine the application that increases the amount and quality of phytochemical content.

EXPERIMENTAL

Biogenic Synthesis of Iron Oxide-NP

Biogenic iron oxide-NPs (BIO-NPs) were obtained using thyme extract. About 1 g dried plant was first infused in 100 mL of boiled water for 20 min and insoluble

macromolecules were removed by filtration (Whatman No. 1). For preparing BIO-NPs, 0.01 M ferrous chloride tetrahydrate and ferric chloride hexahydrate solutions were prepared and mixed in 1:1 (v/v) proportion (Hoang *et al*. 2009). Then, 50 mL of thyme extract was added dropwise onto 50 mL of this mixture (pH: 8). The reaction mixture then turned reddish/brown and was centrifuged to separate the nanoparticles formed (30 min at 6000 rpm). The resultant pellet was dried in a vacuum oven and weighed. The nanoparticles were characterized using UV–Vis (Ultraviolet–Visible), XRD (X-ray powder diffraction), SEM (scanning electron microscopy), and EDS (energy-dispersive x-ray spectroscopy) methods.

Plant Material and Experimental Design

The experiment was performed in a growth chamber under controlled climatic conditions: air temperature of 22 ± 1 °C (day/night), 16 or 8 h, 160 PAR μmol m^{-2} s^{-1}, and 50 ± 10% relative humidity. Seedlings of *Ocimum basilicum* L. (sweet basil) were grown in plastic pots containing a mixture of forest soil. Twenty-day-old seedlings were divided into five groups. Accordingly, exogenous application of BIO-NPs was compared at the following four concentrations: 0.0 mg/L (control: water only), 25 mg/L, 50 mg/L, 100 mg/L, and 200 mg/L (100 mL). All pots were watered weekly for 6 months with 200 mL of water throughout the experiment.

Measurements-Growth Parameters

Relative growth rate (RGR)

Fresh weights of the plants (FMW) from each treatment and dry weights after drying in an oven in 105 °C for 48 h (DMW) were measured. The growth curve of the plants was obtained using the following Eq. 1 (Hunt 1982):

$$RGR\ (\%) = \left[\frac{\mathrm{DMW}}{\mathrm{FMW}}\right] \mathrm{x}\ 100 \quad (1)$$

Leaf area (LA)

Thirty leaf samples from each treatment group were separated from the stem to be used in determining the leaf surface area. The leaf area was calculated according to Pandey and Singh (2011) using the following Eq. 2,

$$\mathrm{LA} = \frac{\mathrm{x}}{y} \quad (2)$$

where *x* denotes graph paper weight of the leaf surface and *y* is the similar graph paper weight of 1 cm^2 area.

Relative water content (RWC)

A total of 0.3 g of leaf samples (FM) were taken from similar points of the plants belonging to each treatment group. To determine the turgid mass (TUM), the samples were kept in petri dishes containing sterile water for 24 h, then they were weighed. The same samples were kept in a pre-heated incubator at 65 °C for 24 h and then weighed to determine the dry weight (DM). Then, RWC was calculated using the Eq. 3 (Salisbury and Ross 1992).

$$\mathrm{RWC}\ (\%) = \left[\frac{\mathrm{FM-DM}}{\mathrm{TUM-DM}}\right] \mathrm{x}\ 100 \quad (3)$$

The stomatal density (SD)

The SD values of the epidermis of leaves was calculated using a number of stomata and epidermal cells counted in each field (1 mm^2) at independent measurement by superficial sections taken from upper and lower surfaces of leaves as described by Rengifo *et al*. (2002). All stomatal parameters were determined (µ) using a calibrated ocular micrometer mounted on a light microscope at a magnification of 40x. Equation 4 is as follows,

$$SD\ (mm^2) = \left[\frac{S}{E+S}\right] \text{ x } 100 \quad (4)$$

where *S* is stomata number and *E* denotes epidermal cells number.

Stomatal Area (SA, μm^2) were determined according to the following equation (Orcen *et al*. 2013) in 50 areas,

$$SA\ (\mu m^2) = \left[\pi \text{ x } \frac{Wg \text{ x } Lg}{4}\right] \quad (5)$$

where *W*g is stomata width (µm) and *L*g is stomata length (µm) were defined as the widest point perpendicular to that axis of the stomata, respectively. Stomata sizes (length and width) were defined (µ) using a calibrated ocular micrometer mounted on a light microscope at a magnification of 40x.

Stomata pore index (SPI), which is defined as the relative measurement of the ratio of the total stomatal pore area of the leaf to the leaf area, was calculated using the stomatal parameters on both surfaces of the leaves of the plants belonging to each treatment group according to Eq. 6 below (Sack *et al*. 2003):

$$SPI = \text{Stomata Density } (SD) \text{x } (\text{Guard Cell Length})^2 \quad (6)$$

The SEM (Leo Stereoscan S-360, Leo, Cambridge, UK) image analysis was used to examine the structures of trichomes and stomata on both surfaces of leaves.

Morphology and distribution of glandular trichomes (peltate and capitate) on both surfaces of the leaves from each treatment were classified as described by Turner *et al*. (2000). To determine the density, trichomes in 50 microscopic fields (1 mm^2) were counted on both surfaces with independent measurements.

The total chlorophyll content in 50 leaves from each treatment were measured using a chlorophyll meter (Minolta SPAD-502; Konica Tokyo, Japan).

Biochemical Parameters

Antioxidant enzyme activities

Leaves (2 g) were ground in liquid nitrogen and homogenized in 10 mL of 50 mM ice-cold sodium phosphate (pH 6.4) containing 0.2 g PVPP for SOD (superoxide dismutase), CAT (catalase), GR (glutathione reductase), and APX (ascorbate peroxidase) extraction. The APX extract contained 1 mM ascorbic acid in addition to the other components of the extraction solution. All homogenates were centrifuged at 15 rpm for 20 min at 4 °C, and the resulting supernatants were stored in the dark at -20 °C until analysis.

The SOD (EC 1.15.1.1) activity was determined by measuring the photochemical reduction reaction capacity of NBT according to the method of Giannopolitis and Ries (1977). The reaction mixture consisted of 0.1 mL supernatant, 2.8 mL reaction buffer (50 mM sodium phosphate buffer (pH 7.8), 13 mM methionine, 75 µM nitroblue tetrazolium (NBT), 0.1 mM EDTA, 50 mM sodium carbonate) and 0.1 mL of 2 mM riboflavin. The test tubes were irradiated under two fluorescent lamps (2 ×15 W) for 15 min, and the

control sample prepared in distilled water was kept in the dark. The absorbance was noted at 560 nm with a spectrophotometer. The 50% inhibition of SOD-inhibitable NBT reduction was taken as one unit of SOD activity.

The method of Chance and Maehly (1955) was used for the CAT (EC 1.11.1.6) activity. The 3 mL reaction mixture consisted of 100 µL of supernatant and 2.9 mL of sodium phosphate buffer (50 mM, pH 7.0) containing 40 mM H_2O_2. Decreasing absorbance for H_2O_2 (ε_{240}= 36 M^{-1} cm^{-1}) was recorded at 240 nm every 30 s for 3 min. One unit of CAT activity was defined as H_2O_2 decomposition per min under standard assay conditions. GR (EC 1.6.4.2) activity was performed following the procedure of Chance and Maehly (1955) with minor modifications. The 350 µL of sodium phosphate buffer (100 mM, pH 7.8) was added to 100 µL of supernatant, followed by 500 µL of 2 mM oxidized glutathione (GSSG). Then, the reaction was started by adding 50 µL of 2.4 mM NADPH solution. The decreasing absorbance of NADPH (ε_{340}= 6.22 mM^{-1} cm^{-1}) in the reaction mixture was determined at intervals of 30, 60, 90, 120, 150 and 180 seconds. One unit of enzyme was defined as the amount of enzyme that caused the oxidation of 1 mmol NADPH per minute at pH 7.8 at 25 °C.

APX (EC 1.11.1.11) activity was determined according to Nakano and Asada (1981). A 700 µL reaction buffer (sodium phosphate buffer (50 mM, pH 7.0), 0.5 mM ascorbate and 0.1 mM EDTA Na_2) and 100 µL of supernatant were added to the reaction tube. The reaction was initiated by adding 200 µL of 1.2 mM H_2O_2 solution. Decreasing absorbance for H_2O_2 (ε_{290}= 2.8 mM^{-1} cm^{-1}) was recorded at 290 nm for 3 min. One unit of APX was defined as the amount of enzyme that caused the decomposition of 1 mmol H_2O_2 per min at pH 7.0 at 25 °C.

All antioxidant enzyme activity was based on protein concentration and protein content was determined with Bradford method (Bradford 1976). All specific antioxidant enzyme activities were expressed as U mg $protein^{-1}$.

H_2O_2 and malondialdehyde contents

Leaves (1 g) were ground in liquid nitrogen and homogenized in 10 mL of 0.1% trichloroacetic acid (TCA) for H_2O_2 (hydrogen peroxide) and malondialdehyde (MDA) extraction. All homogenates were centrifuged at 13 rpm for 20 min at 4 °C, and the resulting supernatants were used directly for the assays. The H_2O_2 content was determined according to the method of Velikova *et al*. (2000). The reaction mixture contained 0.5 mL of 100 mM potassium phosphate buffer (pH 7.0), 2 mL potassium iodide (1 M), and 0.5 mL supernatant. The reaction was developed for 1.0 h in dark. The absorption of the mixture was measured at 390 nm, and water was used as blank. A standard curve was prepared using solutions with known H_2O_2 concentrations. The H_2O_2 content was expressed as µmol g^{-1} FW.

Lipid peroxidation was evaluated by measuring the MDA content according to the method of Heath and Packer (1968). About 1.0 mL of supernatant was added to 4.5 mL of 20% TCA containing 0.5% 2-thiobarbituric acid (TBA), and the mixture was boiled in a water bath for 30 min and then was stopped by cooling the reaction on ice. The mixture was centrifuged at 10 rpm for 10 min, the supernatant absorbance at 532 nm was measured and subtracted from the non-specific absorbance at 600 nm. The amount of MDA-TBA complex was calculated from the extinction coefficient 155 mM^{-1} cm^{-1}.

Phytochemical analysis

For SPME, a polydimethylsiloxane (PDMS)-coated fiber (100 µm) and a Supelco SPME holder were used for sample extraction. The fiber was exposed to the GC (Gas Source) inlet for 30 min for thermal desorption at 22 ± 1 °C before headspace sampling. After the extraction, the SPME fiber was withdrawn from the bottle and inserted into the GC-MS injection port for analysis. The GC-MS analysis was conducted using a gas chromatograph coupled to a mass spectrometer with electron impact ion source. A BP-5 Shimadzu fused silica capillary column (30 m × 0.32 mm i.d., film thickness 0.25 µm) was used for separations. The chromatographic conditions were as follows: the injector and transfer line temperatures were regulated at 140 and 250 °C, respectively; oven temperature was programmed from 35 to 260 °C at 10 °C min^{-1}; carrier gas (helium) flow was 1.4 mL min^{-1}; injection was performed in splitless mode. The quantification of the components was performed based on their total ion current (TIC) GC peak areas on the column. Relative percentage amounts of the separated aromatic compounds were calculated from total ion chromatograms by the computerized integrator.

The phytochemicals identified from all the studied parts of sweet basil were analyzed using LC-10 ADvp pump, SIL–10A Dvpauto-sampler HPLC series (Shimadzu, Kyoto, Japan), and CTO-10 Avp column oven, equipped with a Agilent Eclipse XDB-C18 (250 × 4.60 mm, 5 µm) column. The instrument was operated at 30 ℃, and the flow rate was 0.8 mL min^{-1} and the injection volume was 20 µL. A mobile phase consisting of methanol and acetic acid (3%, v/v) in water were used.

Data Analysis

The obtained data were statistically analyzed using SPSS Software 19. The experiment was repeated in triplicate, and the results expressed as mean ± standard deviation (SD) values. One-way analysis of variance (ANOVA) and Duncan's multiple-range test (DMRT) was used to compare the means of different treatments. Bars showing the same letter(s) are not significantly different ($P \leq 0.05$).

RESULTS AND DISCUSSION

Characterization of BIO-NPs

Optical, structural, and morphological characteristics of green synthesized BIO-NPs were analyzed by UV–Vis, XRD, SEM, and EDS, respectively. The yellowish color of extract prepared from thyme leaves and iron solution mixture changing to reddish/dark brown shows that Fe^{2+} ions reduced to BIO-NPs *via* biological materials. A strong and broad absorption peak centered in the ~400 nm range (Fig. 1a), defined as the characteristic peak of Fe NPs, results from the absorption and scattering of light by Fe_3O_4-NPs (Kejík *et al*. 2021). In addition, the presence of a single peak in the spectrum is also an indicator of the uniformed BIO-NPs. The crystal structure of BIO-NPs obtained with thyme extract was confirmed by XRD results (Fig. 1b). The reflection numbers of (2 2 0), (3 1 1), (2 1 0), (4 0 0), (4 2 2), (5 1 1), and (4 4 0), which correspond to 29.21°, 35.17°, 38.21°, 41.23°, 52.14°, 56.60°, and 62.31° of 2θ values, respectively, defined the peaks of Bragg reflections in the XRD pattern. These matched the magnetite XRD pattern, which describes the crystal structure of the synthesized BIO-NPs. The reflections of the observed peaks explain the crystallization of nanoparticles, and the spinel cubic structure of the formed BIO-NPs (Endla 2022).

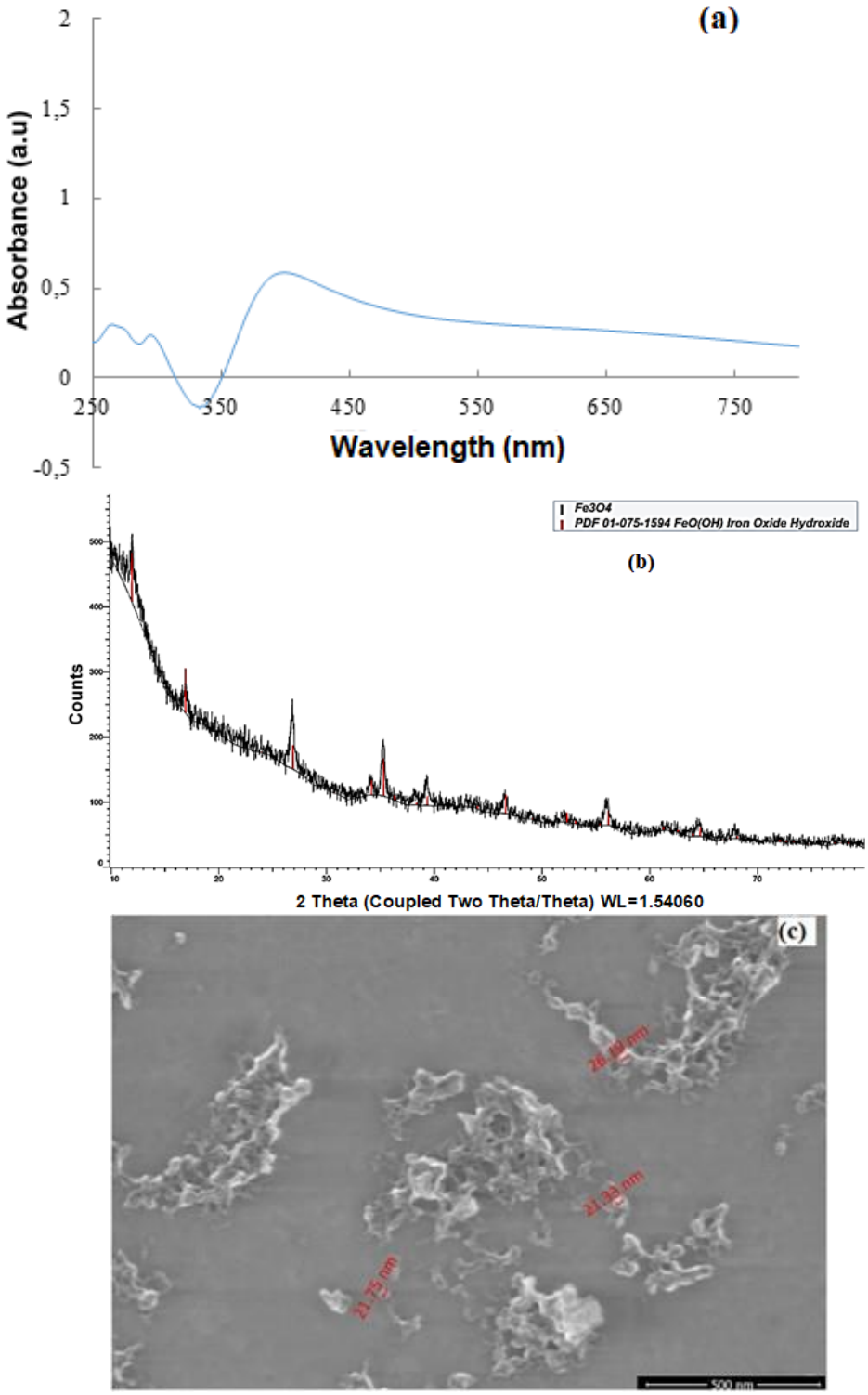
(a)
Absorbance (a.u)
2
1,5
1
0,5
0
-0,5
250
350
450
550
650
750
Wavelength (nm)
Fe3O4
PDF 01-075-1594 FeO(OH) Iron Oxide Hydroxide
(b)
Counts
2 Theta (Coupled Two Theta/Theta) WL=1.54060
(c)
500 nm

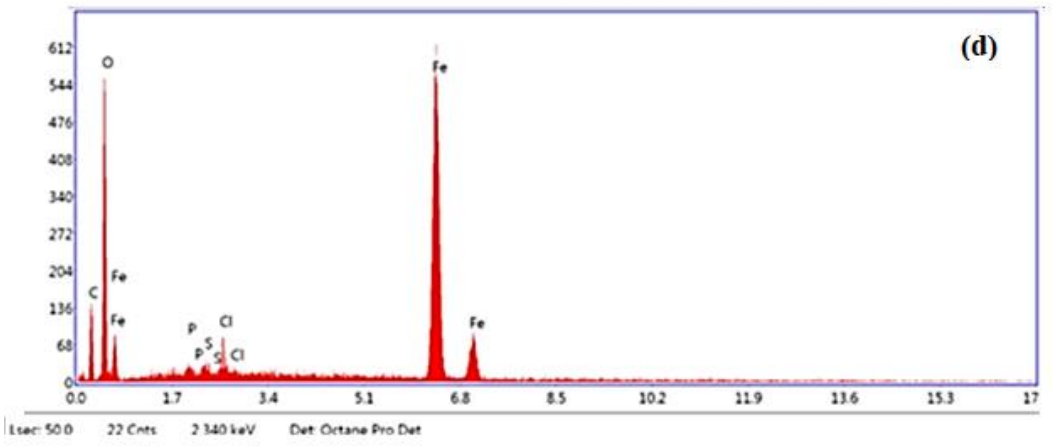

Fig. 1. UV-vis spectra (a); XRD pattern (b); SEM image (c); and EDS spectra (d) of BIO-NPs

The SEM images of biosynthesized BIO-NPs (irregularly shaped, smooth-surfaced, 21 to 27 nm in size) determined that the particles were somewhat agglomerated (Ghereghlou *et al*. 2021) (Fig. 1c). In the EDS spectrum, the presence of a high oxygen (O) peak and strong iron signal indicates BIO-NP formation (Fig. 1d). The presence of nanocrystalline elemental iron (29.69%) with a peak observed at approximately 6 to 7 keV, and the presence of elemental oxygen (44.41%) with a peak at 0.55 keV were confirmed. High oxygen concentration is another indicator confirming the formation of Fe_3O_4-NPs (Anchan *et al*. 2019). The presence of Fe with several peaks, along with other elements, such as Carbon (C), Phosphorus (P), Sulfur (S), and Chlorine (Cl), observed in the EDS spectra and originating from the chemical composition of the plant, indicates that the reduction material can be used as a capping agent.

Traces of BIO-NPs in Growth Biomarkers

Aqueous suspensions of BIO-NPs stimulated the growth of sweet basil seedlings at increasing concentrations. Total chlorophyll content and RGR were highest at 100 mg/L, with 42% and 31% increase rates, respectively. Parallel to the gradual increase in BIO-NPs concentrations, the stimulating effect was reflected in parallel to these parameters. At 200 mg/L, the increase rates of chlorophyll content and RGR decreased 23% and 10%, respectively. However, the stimulating effect of BIO-NPs in RWC did not change with the increase in concentration. The lowest increase was 3% at 50 mg/L, while the highest increase was 5% at 100 mg/L. At 200 mg/L it was reduced 2% compared to control (Fig. 2). The presence of brown spots, defined as toxicity symptoms, on the leaf surfaces of seedlings at 200 mg/L can be considered as a reflection of oxidative stress occurring in leaf cells. The Fe-NPs can provide sufficient iron ions for chlorophyll biosynthesis and redox reactions in chloroplasts. In this way, the chlorophyll content increases, promoting the growth of the plant by increasing the photosynthesis rate and nitrogen fixing capacity. (Zhang *et al.* 2024). The photosynthesis accelerates due to the positive effect of the particle's magnetic field on the enzymatic structures in photosynthesis reactions and plant growth is positively affected, and as NPs produce OH radicals, the cell wall loosens, resulting in increased cell growth (Shah *et al*. 2022).

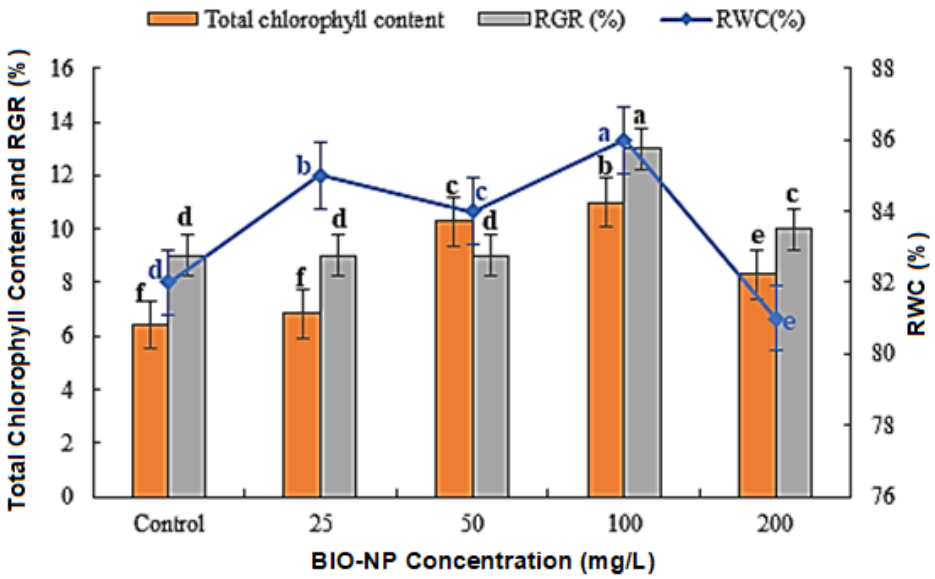

Fig. 2. Effect of BIO-NPs on growth parameters of sweet basil seedlings

Stomata are the only openings of plants derived from the epidermis and are pores through which gas exchange occurs and water balance is maintained through transpiration. Stomata are dynamic with their opening and closing mechanisms. Stomata maintain the balance between CO_2 assimilation and water loss to enable the plant to adapt to changing environmental conditions, enabling photosynthesis and water use efficiency with sustainable productivity (Clark *et al*. 2022). In parallel with the gradual concentration increase of BIO-NPs, differences in the morphological and physiological functions of stomata promote growth of sweet basil at certain NP concentrations. The existence of a negative relationship between stomata density and stomata size (Lawson and Blatt 2014) was defined by the fact that SD was at the highest value and SA was at the lowest value at 100 mg/L in the sweet basil leaves treatment with BIO-NPs. Stomata sizes were smallest at 100 mg/L. The average size of stomata were measured as *W*g 15 µm, and *L*g 19.68 µm. This value was the lowest of all treatments, including the control. In contrast, SD showed the highest value at 25.75 at the same concentration. The fact that SA, defined by stomata sizes, was at its lowest value at this concentration indicates that this was the most active concentration of BIO-NP treatment for growth. Because high SD and low SA mean the presence of many small stomata at high density, a high rate of stomata conductance and photosynthesis rate can be discussed (Wall *et al*. 2022). Because stomata with small guard cells have many ion channels and carriers to move ions, such as potassium, guard cells can regulate water potential and turgor more rapidly and to a greater extent than large stomata. BIO-NPs contributed to the growth of basil seedlings, as the positive effect of stomata conductance in the presence of optimum iron that the plant can use significantly increase the photosynthetic capacity (Amorim *et al*. 2023). At the same time, because the speed and efficiency of stomata movements are inversely proportional to the size of the stomata (McAusland *et al*. 2016), it is understood that the decreasing stoma sizes with gradually increasing BIO-NP application positively affect growth, as fast-moving stomata provide better optimization in gas exchange.

Stomata adjust their opening in response to internal or environmental variables. Stomata pore opening is provided by two guard cells that change cell turgor either actively by pumping ions across the guard cell plasma membrane or passively and reversibly by the

leaf water potential (Buckley 2019). The fact that SPI shows the lowest value at 100 mg/L compared to other treatments (10.01×10^3) and the increase in the size of guard cells is directly proportional to SPI, indicates the presence of small stomata rather than SD (Fig. 3). Optimum water use efficiency is achieved because of the rapid opening and closing capabilities of small stomata (Tsai *et al*. 2022). This variability in the physiological behavior of stomata was an important response to BIO-NP treatment, as it would significantly increase stomata conductance (Durand *et al*. 2020). The stomata pore opening, which determines the rate of entry of CO_2 into the leaves, plays a critical role in directly affecting the photosynthesis mechanism, which is the carbohydrate production process that enables the growth of the plant, as it will maximize carbon uptake in the presence of fast-opening and closing stomata (Lawson and Matthews 2020). Because the conductivity of small stomata during stomata opening is significantly higher than that of larger stomata (Bogeat-Triboulot *et al*. 2019), it may explain the contribution of the relationship between stomata sizes and SPI to plant growth. Because the increase in SPI ratio will increase the total pore area per leaf area, it will cause a low photosynthesis rate with a decrease in the substomatal CO_2 concentration (Bucher *et al*. 2016). Iron is an important microelement in the photosynthetic electron transfer chain and the biosynthesis of chlorophylls (Solymosi and Bertrand 2012). Although it is the fourth most abundant element on earth, most of it is in the Fe^{3+} form in the soil, and because its solubility is quite low, it is the third nutrient element that limits the bioavailability of the plant. It is suggested that the BIO-NPs used in this study increases the bioavailability level of iron and contributes to plant growth and development.

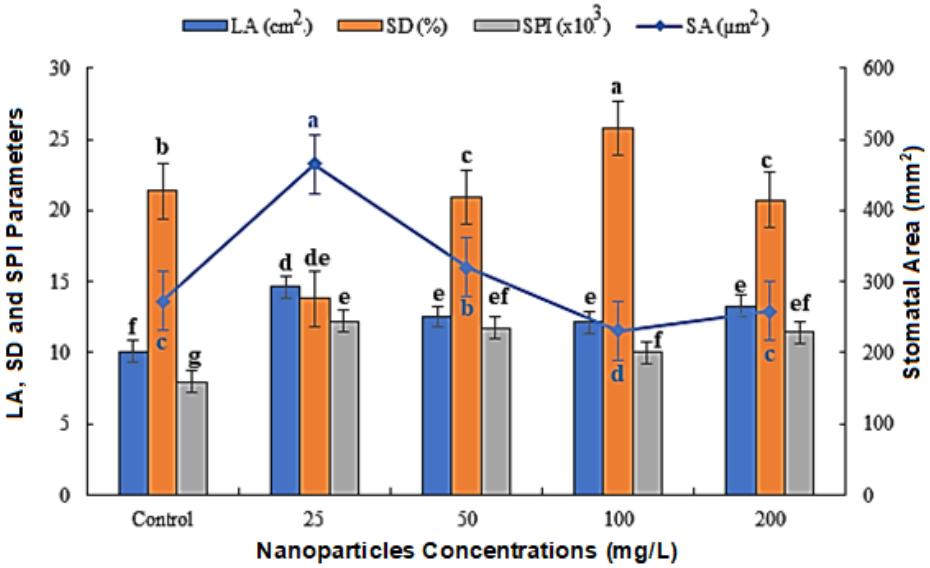

Fig. 3. Effect of BIO-NPs on stomatal movements

Traces of BIO-NPs in Chemical Components of Phytochemicals

The effects of BIO-NP applied at different concentrations on the phytochemical components of sweet basil seedlings were identified by the changes occurring in the peltate and capitate trichomes that produce them.

Phenolic compounds were highest at 50 mg/L BIO-NP. Of these, gallic acid was determined at a higher rate of 71%, and rosmarinic acid 18%, at 50 mg/L compared to the other treatments, compared to the control. Chlorogenic acid was the highest at just 25 mg/L

with a 6% increase. In other treatments, it showed significantly lower values than the control ($P \leq 0.05$). The difference in phenolic amounts varying with BIO-NP concentration was similar to the number of total peltate trichomes (Fig. 4).

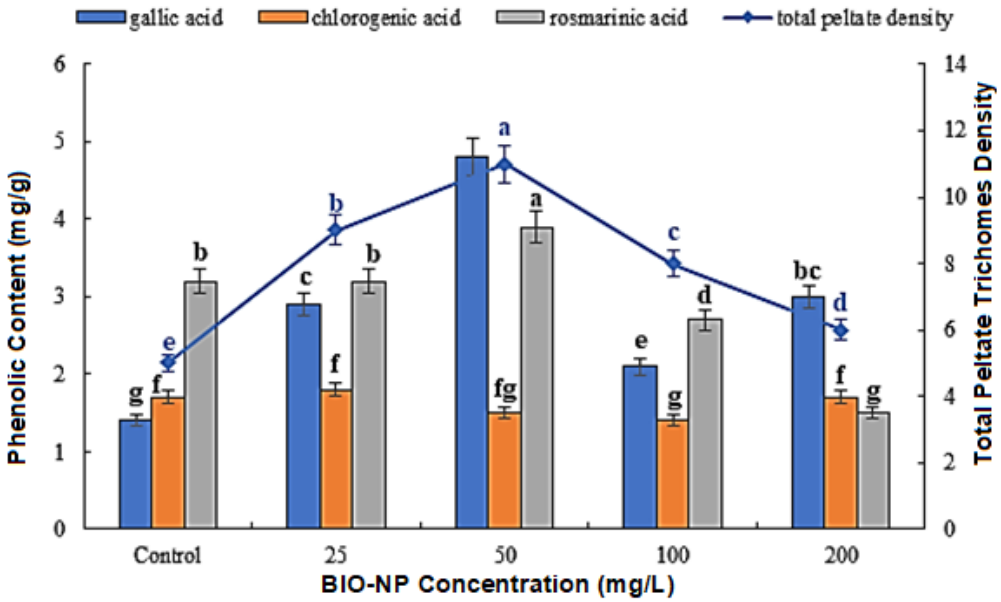

Fig. 4. Effect of BIO-NPs on peltate trichome density and phenolic amount of sweet basil leaves

While the number of peltate trichomes was at the lowest value in the control, the number of peltate trichomes detected in the unit area of 50 mg/L BIO-NP sweet basil leaves was higher than the other treatments, with a 55% increase. In other treatments, a parallel decrease was observed with the increase in BIO-NP concentration. Peltate trichomes are formed by a disc-shaped arrangement of four secretory cells covered with a fat sac membrane. Synthesis and storage of phenolic substances occur only in peltate trichomes (Tang *et al*. 2022), because these structures are active in the leucoplasts of peltate trichomes in leaves, where the majority of enzyme activities in the biosynthetic pathway of phytochemicals are located (Turner and Croteau 2004). The linear relationship between the density of peltate trichomes and the amount and content of essential oil of the plant has also been determined by the researchers. For example, when different concentrations of metal oxide nanoparticles were applied to the mint plant, it was determined that the increase in the amount and quality of essential oil at 150 mg/L was directly proportional to the diameter and number of peltate trichomes (Ahmad *et al*. 2018). In another study, when the effect of different concentrations of SiONPs was examined, a significant increase was found in the diameter and number of peltate trichomes at 50 and 100 mg/L, while the amount of essential oil reached the highest value with 26.5% at the same concentration (Ahmad *et al*. 2020).

The use of BIO-NPs increased the density of peltate trichomes and also provided a significant increase in the amount of phytochemicals (Fig. 5).

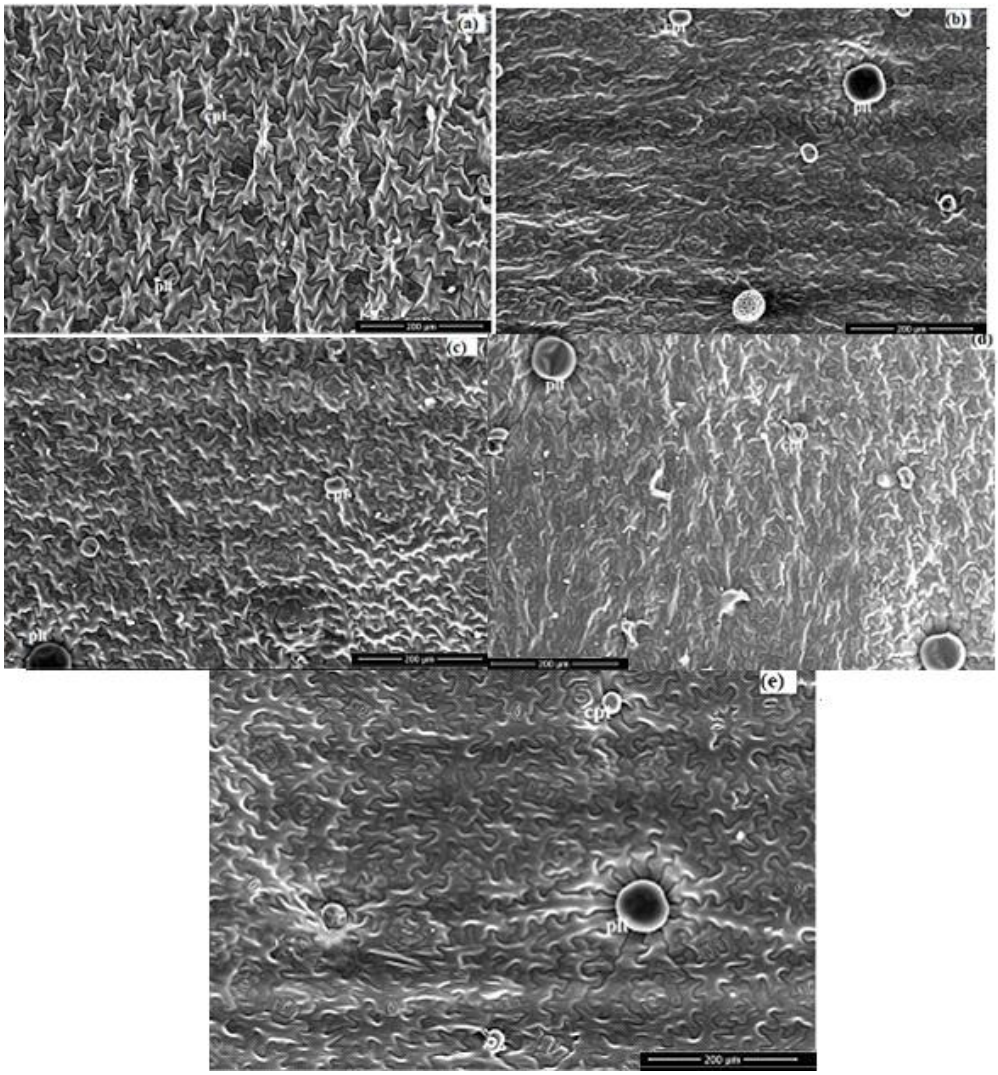

Fig. 5. Effect of BIO-NPs on glandular trichomes; a: Control, b: 25 mg/L, c: 50 mg/L, d: 100 mg/L, e: 200 mg/L (plt: peltate trichomes, cpt: capitate trichomes)

This increase was due to the contribution of capitate trichomes as well as peltate trichomes. Capitate trichomes consist of a stem consisting of one or a few cells attached to the leaf surface and a head consisting of one or two cells. According to GC/MS results, approximately 98 phytochemicals were determined in sweet basil leaves. The most variable ones were evaluated. While the BIO-NP concentration difference changed the amount of phytochemical, the total number of trichomes was also different ($P \leq 0.05$). The total number of trichomes was highest at 100 mg/L. Only α-pinene showed a maximum increase at 50 mg/L and α-humulene showed a maximum increase at 200 mg/L. Other phytochemicals were at the highest value at 100 mg/L. At this concentration, the direct proportion between the increase in phytochemical rate and total trichomes may indicate that BIO-NP treatment promotes the amount of phytochemical by increasing the number of trichomes.

The positive effect of BIO-NPs on the biosynthesis of phytochemicals was further confirmed when BIO-NP contents reached optimum level in cells, which can increase the phytochemical amount of basil leaves by increasing the activation of some enzymes such as (R)-linalool synthase (LIS), geraniol synthase (Iijima *et al*. 2004). There are also

phytochemicals whose percentages decrease compared to the control. In fact, some phytochemicals were detected in the control group but were not found as application concentrations increased. For example, methyl benzoate decreased 78% compared to the control group at 25 mg/L BIO-NP concentration and was not detected at other concentrations. Similarly, methyl salicylate decreased 80% at the same concentration compared to the control but could not be detected at other concentrations. 1-Octen-3-yl acetate decreased 25%, 44%, 50%, and 60%, at 25, 50, 100, 200 mg/L BIO-NP concentrations, respectively, compared to control (Fig. 6). Methyl benzoate and methyl salicylate are volatile methyl esters that attract pollinators by contributing to the aroma of flowers and provide communication between plants during pathogen infection (Negre *et al*. 2002). However, the substantial increase in other volatile compounds with the BIO-NP concentration indicates that the essential oil quality in sweet basil leaves had increased significantly.

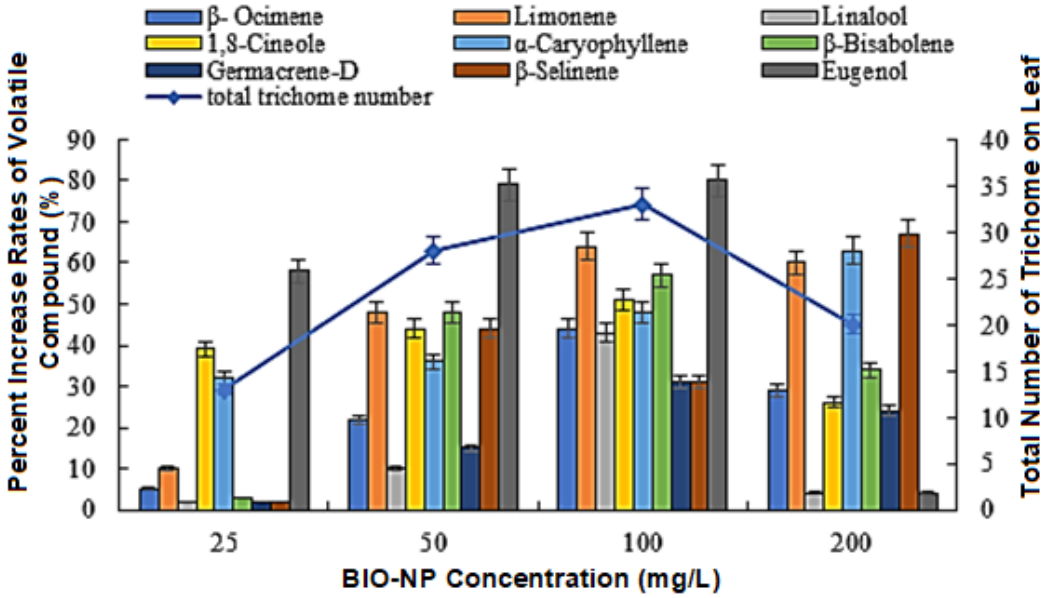

Fig. 6. Effect of BIO-NPs on phytochemical contents and glandular trichomes of sweet basil leaves

Traces of BIO-NPs in Antioxidant Enzymes, MDA, and H_2O_2 Content

The CAT, GR, and APX activities were affected by BIO-NPs treatments. A noticeable increase in CAT and APX activities compared to the control was observed for 50 mg/L (Fig. 7). The SOD activity values were around 2.4 to 3.0 U mg^{-1} protein and showed no noticeable difference between control and any of NPs treatments. The SOD dismutase is a crucial part of plants' antioxidant defense system. It is a significant superoxide (O_2^-) scavenger, and because of its enzymatic activity, H_2O_2 and O_2 are produced. The SOD appears crucial in protecting plants from oxidative stress. Several reports have recorded that increased SOD activity is associated with an increase in plants' tolerance to environmental stress, such as NP toxicity; this means that SOD can act as an indirect selection criterion for investigating oxidative stress (Zhang *et al*. 2017). The slight increase in SOD activity suggests that BIO-NPs might improve the stress tolerance in sweet basil by mediating the metabolic pathway of redox. The SOD activity was also almost equal in 25, 50, 100, and 200 mg/L BIO-NPs-treated plants. No statistically significant difference in SOD activity was observed between the control plants and those treated with

NP solution. Among all BIO-NPs concentrations, the highest value of SOD activity was recorded in plants treated with 25 mg/L of BIO-NPs (3.055 U mg protein^{-1}), while lowest activity was at 200 mg/L (2.763 U mg protein^{-1}).

The CAT is a large enzyme that catalyzes the dismutation of two H_2O_2 molecules to water and oxygen and contains heme-bound iron in its active sites (Sharma *et al*. 2012b). Because CAT, peroxidase, and APX enzymes contain iron porphyrin, which has a special role as prosthetic groups in plant metabolism, their activity may decrease in cases of iron deficiency (Sun *et al*. 2007). BIO-NPs treatments increased CAT activity at all concentrations compared with controls, but statistically significant differences were only shown in 50 mg/L (0.995 U mg protein^{-1}) and 200 mg/L (0.973 U mg protein^{-1}). Similar reactions of *Brassica juncea* to silver nanoparticles were also mentioned by Sharma *et al*. (2012a). Higher CAT activity may be due to higher production of ROS and thereby greater scavenging of ROS to reduce the ROS mediated damage to the plants.

According to research, the Asc-GSH cycle's rate-limiting enzyme is GR, which catalyzes the conversion of GSSG to GSH using the electron donor NADPH. Therefore, increasing GR as a result of re-reducing oxidized glutathione is crucial (Rao and Reddy 2008). The results obtained in Fig. 7 show that the foliar application of BIO-NPs on sweet basil plants decreased the activities of GR enzymes in comparison with control plants. All concentrations of BIO-NPs decreased the GR activity. The GR enzyme activity decreased 25%, 9%, 10%, and 22% at 25, 50, 100, and 200 mg/L of BIO-NP, respectively, compared to the control plants. The glutathione-ascorbate cycle plays an important role in the development of the defense system against oxidative stress (Khanna-Chopra and Selote 2007). It is obvious that the applied BIO-NP concentrations do not cause stress in the plant because the increase in GR activities under stress conditions will cause a decrease in the effects of oxidative stress.

The APX, a key element of the AsA-GSH cycle, is crucial for the regulation of intracellular ROS levels. In plant cells, APX is one of the most widely present antioxidant enzymes and plays a significant role in scavenging of H_2O_2 (Sarker and Oba, 2018). The APX activity of sweet basil increased with the BIO-NPs increase when the BIO-NPs concentration was lower than 50 mg/L, and the APX activity decreased when the BIO-NPs concentration was higher than 50 mg/L. The APX activity significantly increased in plants treated with 25 mg/L (36.751 U mg protein^{-1}) and 50 mg/L (43.613 U mg protein^{-1}) BIO-NPs in comparison to untreated plants. The APX activity reached maximum activity at 50 mg/L but decreased significantly in response to increasing BIO-NPs concentrations, with the lowest activity at 200 mg/L (15.263 U mg protein^{-1}). When the BIO-NP concentration was higher than 50 mg/L, the H_2O_2 and OH^- scavenging capacity of APX activity decreased and the antioxidant defense system was restricted.

The MDA is a marker of membrane damage that is produced as a result of lipid peroxidation (Sharma *et al*. 2012b). Among all concentrations of BIO-NPs, treatment with 200 mg/L caused maximal decrease in MDA content in comparison to untreated plants (Fig. 7). The MDA content in plants treated with 25 mg/L (2.827 nmol g^{-1}), 50 mg/L (2.862 nmol g^{-1}), 100 mg/L (2.839 nmol g^{-1}), and 200 mg/L (2.531 nmol g^{-1}) BIO-NPs was significantly lower than the untreated plants. Irrespective of the concentration of BIO-NPs used, the treated plants always accumulated lesser MDA contents than the control plants. This clearly shows that BIO-NPs treatment might increase the effectiveness of electron exchange/transport reactions and successfully reduce the oxidative load in the treated plants (Joshi *et al*. 2011). Similar to this study, iron oxides at 2 to 50 mg/L concentrations

were not toxic in *Citrus maxima* plants, and low MDA levels were beneficial in preserving cell membrane structure and function (Li *et al*. 2013).

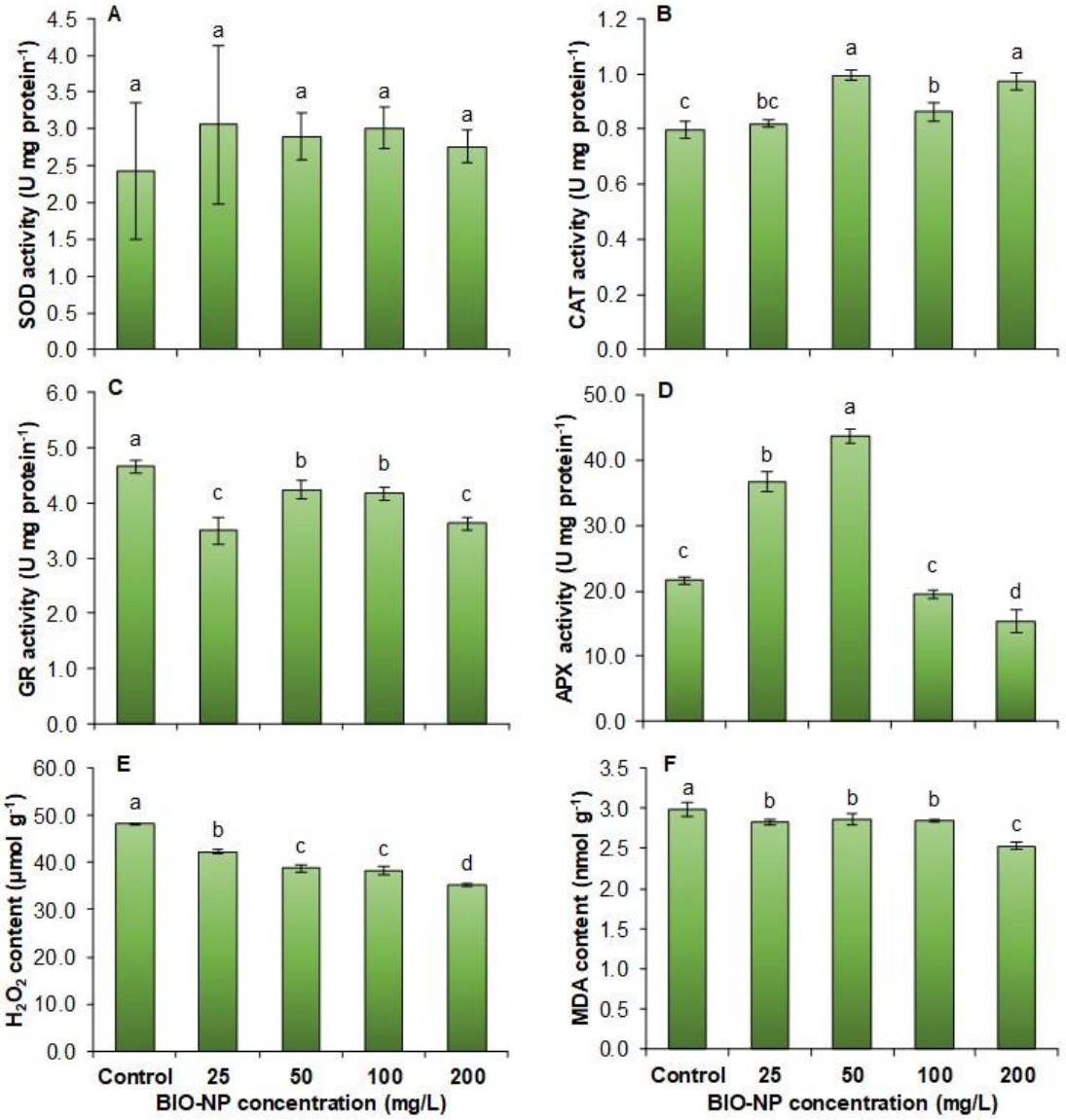

Fig. 7. Effects of seed treatment with various concentrations of BIO-NPs on the activity of antioxidant enzymes: SOD (A), CAT (B), GR (C), APX (D), H_2O_2 content (E), and MDA content (F) in leaves of sweet basil plants. Data labelled with different lower-case letters are significantly different at $p < 0.05$

H_2O_2, being one of the most toxic forms of active oxygen, serves as a crucial secondary messenger for activating defense-related responses as well as growth promontory in plants (Mittler *et al*. 2004). Under normal development conditions as well as a variety of stressful circumstances, H_2O_2 is produced in cells. In addition to being a ROS, it is also regarded as a signaling molecule that promotes tolerance to a variety of environmental stresses and is involved in the control of biological processes (Sharma *et al*. 2012). In this study's experiments a drastic reduction in H_2O_2 content was recorded in plants treated with 25 mg/L BIO-NP (42.3 µmol g^{-1}), as compared to the control plants (Fig. 7). With further increase in the concentration of BIO-NPs, the level of H_2O_2 decreased steadily. A 27% lower H_2O_2 level was recorded in the plants treated with 200 mg/L BIO-

NPs solution (35.3 µmol g^{-1}). These results suggest that BIO-NPs trigger the cellular antioxidant system *via* the H_2O_2 signaling pathway, as H_2O_2 controls the expression of several genes, including those that encode antioxidant enzymes and H_2O_2 metabolism regulators (Slesak *et al*. 2007).

The result of Pearson linear correlation analysis based on the effect of different concentration treatments of BIO-NPs is provided in Fig. 8. Among the three significant coefficients, both were negatively correlated with each other. The GR activity was negatively correlated with LA r = -0.95) and SD showed significant ($P \leq 0.01$) negative correlation with SA (r = -0.94). The LA was positively correlated with SPI (r = 0.93). When morphological and biochemical data were compared, the SOD activity showed a positive correlation with PD (r = 0.73) and LA (r = 0.79) parameters. Additionally, PD showed positive correlation with APX activity (r = 0.86). The GR and SPI were negatively correlated with each other (r = 0.82).

Fig. 8. Relationships and correlations between antioxidant enzyme activities generated by Heat map using mean values obtained from sweet basil after BIO-NPs treatment. Color scale displays the intensity of normalized mean values of different parameters

CONCLUSIONS

1. Due to the role of biogenic iron oxide nanoparticles (BIO-NPs) in increasing growth and biomass in basil, the physiological results from this study showed that the BIO-NPs were effective on growth biomarkers, polyphenolic compounds, volatile compounds, antioxidant enzymes, and biochemical contents, but these effects were concentration-dependent.
2. Total chlorophyll content, dry weight, relative water content, stomatal density, volatile components, and total trichome density in basil increased significantly in response to 100 mg/L BIO-NP treatment.

3. While SOD activity did not change significantly over BIO-NP concentrations, 50 mg/L BIO-NP significantly increased CAT and APX activities and reduced the damaging effects of cellular oxidation. In addition, 200 mg/L BIO-NP significantly reduced the H_2O_2 and MDA contents. Therefore, oxidative stress control is an important component of the plant's ability to withstand environmental stress and to succeed in peltate trichome density, and growth biomarkers.
4. The results will help answer the question of what physiological and biochemical changes BIO-NPs causes in basil. However, it is necessary to measure the iron content in basil tissues after BIO-NP treatment, and further studies are needed to examine the transport and interaction mechanism between BIO-NPs and plant tissues at the cellular and molecular levels.

REFERENCES CITED

Ahmad, B., Khan, M. M. A., Jaleel, H., Shabbir, A., Sadiq, Y., and Uddin, M. (2020). "Silicon nanoparticles mediated increase in glandular trichomes and regulation of photosynthetic and quality attributes in *Mentha piperita* L.," *J. Plant Growth Regul.* 39, 346-357. DOI: 10.1007/s00344-019-09986

Ahmad, B., Shabbir, A., Jaleel, H., Khan, M. M. A., and Sadiq, Y. (2018). "Efficacy of titanium dioxide nanoparticles in modulating photosynthesis, peltate glandular trichomes and essential oil production and quality in *Mentha piperita* L.," *Curr. Plant Biol.* 13, 6-15. DOI: 10.1016/j.cpb.2018.04.00

Alkhatib, R., Alkhatib, B., Abdo, N., Al-Eitan, L., and Creamer, R. (2019). "Physio-biochemical and ultrastructural impact of (Fe_3O_4) nanoparticles on tobacco," *BMC Plant Biol.* 19(1), article 253. DOI: 10.1186/s12870-019-1864-1

Amorim, F. F. V. R. D., Natale, W., Taniguchi, C. A. K., Serrano, L. A. L., Corrêa, M. C. D. M., and Artur, A. G. (2023). "Iron doses on growth and gas exchange of dwarf cashew seedlings," *J. Plant Nutr.* 46(10), 2315-2328. DOI: 10.1080/01904167.2022.2155532.

Anchan, S., Pai, S., Sridevi, H., Varadavenkatesan, T., Vinayagam, R., and Selvaraj, R. (2019). "Biogenic synthesis of ferric oxide nanoparticles using the leaf extract of *Peltophorum pterocarpum* and their catalytic dye degradation potential," *Biocatal. Agric. Biotechnol.* 20, article ID 101251. DOI: 10.1016/j.bcab.2019.101251

Bogeat-Triboulot, M. B., Buré, C., Gerardin, T., Chuste, P. A., Le Thiec, D., Hummel, I., Durand, M., Wildhagen, H., Douthe, C., Molins, A., *et al.* (2019). "Additive effects of high growth rate and low transpiration rate drive differences in whole plant transpiration efficiency among black poplar genotypes," *Environ. Exp. Bot.* 166, article ID 103784. DOI: 10.1016/j.envexpbot.2019.05.021

Bradford, M. M. (1976). "A rapid and sensitive method for the quantitation of microgram quantities of protein utilizing the principle of protein-dye binding," *Anal. Biochem.* 72(1-2), 248-254. DOI: 10.1016/0003-2697(76)90527-3

Bucher, S. F., Auerswald, K., Tautenhahn, S., Geiger, A., Otto, J., Müller, A., and Römermann, C. (2016). "Inter-and intraspecific variation in stomatal pore area index along elevational gradients and its relation to leaf functional traits," *Plant Ecol.* 217, 229-240. DOI: 10.1007/s11258-016-0564-2

Buckley, T. N. (2019). "How do stomata respond to water status?," *New Phytol*. 224(1), 21-36. DOI: 10.1111/nph.15899

Chance, B., and Maehly, A. C. (1955). "Assay of catalases and peroxidases," *Method. Enzymol.* 2, 764-775. DOI: 10.1016/S0076-6879(55)02300-8

Clark, J. W., Harris, B. J., Hetherington, A. J., Hurtado-Castano, N., Brench, R. A., Casson, S., Williams, T. A., Gray, J. E., and Hetherington, A. M. (2022). "The origin and evolution of stomata," *Curr. Biol*. 32(11), R539-R553. DOI: 10.1016/j.cub.2022.04.040

Durand, M., Brendel, O., Buré, C., Courtois, P., Lily, J. B., Granier, A., and Le Thiec, D. (2020). "Impacts of a partial rainfall exclusion in the field on growth and transpiration: Consequences for leaf-level and whole-plant water-use efficiency compared to controlled conditions," *Agric. For Meteorol.* 282, article ID 107873. DOI: 10.1016/j.agrformet.2019.107873

Endla, P. (2022). "Fabrication and characterization of iron (Fe) nanoparticles by Hall-Williamson, ball milling and X-ray diffraction method," *Mater. Today Proc.* 68(5), 1571-1574. DOI: 10.1016/j.matpr.2022.07.239

Feng, Y., Kreslavski, V. D., Shmarev, A. N., Ivanov, A. A., Zharmukhamedov, S. K., Kosobryukhov, A., Yu, M., Allakhverdiev, S., and Shabala, S. (2022). "Effects of iron oxide nanoparticles (Fe_3O_4) on growth, photosynthesis, antioxidant activity and distribution of mineral elements in wheat (*Triticum aestivum*) plants," *Plants* 11(14), article 1894. DOI: 10.3390/plants11141894

Ghereghlou, M., Esmaeili, A. A., and Darroudi, M. (2021). "Preparation of Fe_3O_4@ C-dots as a recyclable magnetic nanocatalyst using *Elaeagnus angustifolia* and its application for the green synthesis of formamidines," *Appl. Organomet. Chem.* 35(11), article ID e6387. DOI: 10.1002/aoc.6387

Giannopolitis, C. N., and Ries, S. K. (1977). "Superoxide dismutases: I. Occurrence in higher plants," *Plant Physiol.* 59(2), 309-314. DOI: 10.1104/pp.59.2.309

Heath, R. L., and Packer, L. (1968). "Photoperoxidation in isolated chloroplasts: I. Kinetics and stoichiometry of fatty acid peroxidation," *Arch. Biochem. Biophys.* 125(1), 189-198. DOI: 10.1016/0003-9861(68)90654-1

Hoag, G. E., Collins, J. B., Holcomb, J. L., Hoag, J. R., Nadagouda, M. N., and Varma, R. S. (2009). "Degradation of bromothymol blue by 'greener'nano-scale zero-valent iron synthesized using tea polyphenols," *J. Mater. Chem.* 19(45), 8671-8677. DOI: 10.1039/B909148c

Hunt, R. (1982). "Plant growth curves," in: *The Functional Approach to Plant Growth Analysis*, Edward Arnold Ltd., London, UK, pp. 248.

Iijima, Y., Davidovich-Rikanati, R., Fridman, E., Gang, D. R., Bar, E., Lewinsohn, E., and Pichersky, E. (2004). "The biochemical and molecular basis for the divergent patterns in the biosynthesis of terpenes and phenylpropenes in the peltate glands of three cultivars of basil," *Plant Physiol.* 136(3), 3724-3736. DOI: 10.1104/pp.104.051318

Joshi, P. K., Saxena, S. C., and Arora, S. (2011). "Characterization of *Brassica juncea* antioxidant potential under salinity stress," *Acta Physiol. Plant.* 33(3), 811-822. DOI: 10.1007/s11738-010-0606-7

Kejík, Z., Kaplánek, R., Masařík, M., Babula, P., Matkowski, A., Filipenský, P., Pilipenský, P., Veselá, K., Gburek, J., Sykora, D., *et al.* (2021). "Iron complexes of flavonoids-antioxidant capacity and beyond," *Int. J. Mol. Sci.* 22(2), article 646. DOI: 10.3390/ijms22020646

Khanna-Chopra, R., and Selote, D. S. (2007). "Acclimation to drought stress generates oxidative stress tolerance in drought-resistant than susceptible wheat cultivar under field conditions," *Environ. Exp. Bot.* 60, 276-283. DOI: 10.1016/j.envexpbot.2006.11.004

Kruszka, D., Selvakesavan, R. K., Kachlicki P., and Franklin, G. (2022). "Untargeted metabolomics analysis reveals the elicitation of important secondary metabolites upon treatment with various metal and metal oxide nanoparticles in *Hypericum perforatum* L. cell suspension cultures," *Ind. Crop. Prod.* 178, article ID 114561. DOI: 10.1016/j.indcrop.2022.114561

Lawson, T., and Blatt, M. R. (2014). "Stomatal size, speed, and responsiveness impact on photosynthesis and water use efficiency," *Plant Physiol.* 164(4), 1556-1570. DOI: 10.1104/pp.114.237107

Lawson, T., and Matthews, J. (2020). "Guard cell metabolism and stomatal function," *Annual Review of Plant Biol.* 71, 273-302. DOI: 10.1146/annurev-arplant-050718-100251

Li, J., Chang, P. R., Huang, J., Wang, Y., Yuan, H., and Ren, O. (2013). "Physiological effects of magnetic iron oxide nanoparticles towards watermelon," *J. Nanosci. Nanotechno.* 13, 5561-5567. DOI: 10.1166/jnn.2013.7533

Macera, L., Taglieri, G., Daniele, V., Passacantando, M., and D'Orazio, F. (2020). "Nano-sized Fe (III) oxide particles starting from an innovative and eco-friendly synthesis method, *Nanomaterials* 10(2), 323. DOI: 10.3390/nano10020323

McAusland, L., Vialet-Chabrand, S., Davey, P., Baker, N. R., Brendel, O., and Lawson, T. (2016). "Effects of kinetics of light-induced stomatal responses on photosynthesis and water-use efficiency," *New Phytol.* 211(4), 1209-1220. DOI: 10.1111/nph.14000

Mittler, R., Vanderauwera, S., Gollery, M., and Van, B. F. (2004). "Reactive oxygen gene network of plant," *Trends Plant Sci.* 9, 490-498. DOI: 10.1016/j.tplants.2004.08.009

Morales, F., Ancín, M., Fakhet, D., González-Torralba, J., Gámez, A. L., Seminario, A., Soba, D., Mariem, S. B., Garriga, M., and Aranjuelo, I. (2020). "Photosynthetic metabolism under stressful growth conditions as a bases for crop breeding and yield improvement," *Plants* 9(1), article 88. DOI: 10.3390/plants9010088

Nakano, Y., and Asada, K. (1981). "Hydrogen peroxide is scavenged by ascorbate-specific peroxidase in spinach chloroplasts," *Plant Cell Physiol.* 22(5), 867-880. DOI: 10.1093/oxfordjournals.pcp.a076232

Negre, F., Kolosova, N., Knoll, J., Kish, C. M., and Dudareva, N. (2002). "Novel S-adenosyl-L-methionine: salicylic acid carboxyl methyltransferase, an enzyme responsible for biosynthesis of methyl salicylate and methyl benzoate, is not involved in floral scent production in snapdragon flowers," *Arch. Biochem. Biophys.* 406(2), 261-270. DOI: 10.1016/S0003-9861(02)00458-7

Nozoe, T., Tachibana, M., Uchino, A., and Yokogami, N. (2009). "Effects of ferrous iron (Fe) on the germination and root elongation of paddy rice and weeds," *Weed Boil. Manag.* 9(1), 20-26. DOI: 10.1111/j.1445-6664.2008.00314.x

Orcen, N., Nazarian, G., and Gharibkhani, M. (2013). "The responses of stomatal parameters and SPAD value in Asian tobacco exposed to chromium," *Pol. J. Environ. Stud.* 22, 1441-1447.

Pandey, S. K., and Singh, H. (2011). "A simple, cost-effective method for leaf area estimation," *J. Bot.* 2011, article ID 658240. DOI: 10.1155/2011/658240

Poddar, K., Sarkar, D., and Sarkar, A. (2020). "Nanoparticles on photosynthesis of plants: effects and role," in: *Green Nanoparticles: Synthesis and Biomedical Applications*, Springer Nature, Cham, Switzerland, pp. 273-287.

Rani, N., Kumari, K., Sangwan, P., Barala, P., Yadav, J., and Vijeta Hooda, V. (2022). "Nano-iron and nano-zinc induced growth and metabolic changes in *Vigna radiata*," *Sustainability* 14(14), article 8251. DOI: 10.3390/su14148251

Ranjan, A., Rajput, V. D., Kumari, A., Mandzhieva, S. S., Sushkova, S., Prazdnova, E. V., Zargar, S. M., Raza, A., Minkina, T., and Chung, G. (2022). "Nanobionics in crop production: An emerging approach to modulate plant functionalities," *Plants* 11(5), article 692. DOI: 10.3390/plants11050692

Rao, A. S. V. C., and Reddy, A. (2008). "Glutathione reductase: a putative redox regulatory system in plant cells," in: *Sulfur Assimilation and Abiotic Stresses in Plants*, N. A. Khan, S. Singh, and S. Umar (Eds.), Springer-Verlag, Berlin Heidelberg, Germany, pp. 111-147.

Rengifo, E., Urich, R., and Herrera, A. (2002). "Water relations and leaf anatomy of the tropical species, *Jatropha gossypifolia* and *Alternanthera crucis*, grown under elevated CO_2 concentration," *Photosynthetica* 40, 397-403.

Sack, L., Cowan, P. D., Jaikumar, N., and Holbrook, N. M. (2003). "The 'hydrology' of leaves: Co-ordination of structure and function in temperate woody species," *Plant Cell Environ.* 26(8), 1343-1356. DOI: 10.1046/j.0016-8025.2003.01058.x

Salisbury, B., and Ross, W. (1992). *Plant Physiology*, 4th Ed., Wadsworth, Belmont, CA, pp. 682.

Sarker, U., and Oba, S. (2018). "Catalase, superoxide dismutase and ascorbate-glutathione cycle enzymes confer drought tolerance of *Amaranthus tricolor*," *Sci. Rep.* 8(1), article ID 16496. DOI: 10.1038/s41598-018-34944-0

Shah, A. A., Yasin, N. A., Mudassir, M., Ramzan, M., Hussain, I., Siddiqui, M. H., Ali, H. M., Shabbir, Z., Ali, A., Ahmed, S., *et al.* (2022). "Iron oxide nanoparticles and selenium supplementation improve growth and photosynthesis by modulating antioxidant system and gene expression of chlorophyll synthase (CHLG) and protochlorophyllide oxidoreductase (POR) in arsenic-stressed *Cucumis melo*," *Environm. Pollut.* 307, article ID 119413. DOI: 10.1016/j.envpol.2022.119413

Sharma, P., Jha, A. B., Dubey, R. S., and Pessarakli, M. (2012b). "Reactive oxygen species, oxidative damage, and antioxidative defense mechanism in plants under stressful conditions," *J. Bot.* 26. article ID 217037. DOI: 10.1155/2012/217037

Sharma, P., Bhatt, D., Zaidi, M. G. H., Saradhi, P. P., Khanna, P. K., and Arora, S. (2012a). "Silver nanoparticle mediated enhancement in growth and antioxidant status of *Brassica juncea*," *Appl. Biochem. Biotech.* 167, 2225-2233. DOI: 10.1007/s12010-012-9759-8

Slesak, I., Libik, M., Karpinska, B., Karpinski, S., and Miszalski, Z. (2007). "The role of hydrogen peroxide in regulation of plant metabolism and cellular signaling in response to environmental stresses," *Acta Biochim. Pol.* 54(1), 39-50. DOI:

Solymosi, K., and Bertrand, M. (2012). "Soil metals, chloroplasts, and secure crop production: A review," *Agron. Sustain. Dev.* 32, 245-272. DOI: 10.1007/s13593-011-0019-z

Sun, B., Jing, Y., Chen, K., Song, L., Chen, F., and Zhang, L. (2007). "Protective effect of nitric oxide on iron deficiency-induced oxidative stress in maize (*Zea mays*)," *J. Plant Physiol.* 164(5), 536-543. DOI: 10.1016/j.jplph.2006.02.011

Tang, H. M., Jiang, Q., Liu, H. Y., Zhang, F., Liu, Q., Pu, G. B., and Zhang, Y. Q. (2022). "Glandular trichomes of medicinal plants: Types, separation and purification, biological activities," *Biol. Plant.* 66, 219-227. DOI: 10.32615/bp.2022.027

Tsai, M. Y., Kuan, C., Guo, Z. L., Yang, H. A., Chung, K. F., and Ho C. M. K. (2022). "Stomatal clustering in Begonia improves water use efficiency by modulating stomatal movement and leaf structure," *Plant Environ. Interact.* 3(4), 141-154. DOI: 10.1002/pei3.10086

Turner, G. W., Gershenzon, J., and Croteau, R. B. (2000). "Development of peltate glandular trichomes of peppermint," *Plant Physiol.* 124, 665-680. DOI: 10.1104/pp.124.2.665

Turner, G. W., and Croteau, R. (2004). "Organization of monoterpene biosynthesis in Mentha. Immunocytochemical localizations of geranyl diphosphate synthase, limonene-6-hydroxylase, isopiperitenol dehydrogenase, and pulegone reductase," *Plant Physiol.* 136(4), 4215-4227. DOI: 10.1104/pp.104.050229

Velikova, V., Yordanov, I., and Edreva, A. J. P. S. (2000). "Oxidative stress and some antioxidant systems in acid rain-treated bean plants: Protective role of exogenous polyamines," *Plant Sci.* 151(1), 59-66. DOI: 10.1016/S0168-9452(99)00197-1

Wall, S., Vialet-Chabrand, S., Davey, P., Van Rie, J., Galle, A., Cockram, J., and Lawson, T. (2022). "Stomata on the abaxial and adaxial leaf surfaces contribute differently to leaf gas exchange and photosynthesis in wheat," *New Phytol.* 235(5), 1743-1756. DOI: 10.1111/nph.18257

Zahra, N., Hafeez, M. B., Shaukat, K., Wahid, A., and Hasanuzzaman, M. (2021). "Fe toxicity in plants: Impacts and remediation," *Physiol. Plant.* 173(1), 201-222, article ID 33547807. DOI: 10.1111/ppl.13361

Zawadzka, K., Felczak, A., Nowak, M., Kowalczyk, A., Piwoński, I., and Lisowska, K. (2021). "Antimicrobial activity and toxicological risk assessment of silver nanoparticles synthesized using an eco-friendly method with *Gloeophyllum striatum*," *J. Hazard. Mater.* 418, article ID 126316. DOI: 10.1016/j.jhazmat.2021.126316

Zhang, S., Yi, K., Chen, A., Shao, J., Peng, L., and Luo, S. (2022). "Toxicity of zero-valent iron nanoparticles to soil organisms and the associated defense mechanisms: A review," *Ecotoxicol.* 31(6), 873-883. DOI: 10.1007/s10646-022-02565-z

Zhang, P., Ma, Y., Liu, S., Wang, G., Zhang, J., He, X., Zhang, J., Rui, Y., and Zhang, Z. (2017). "Phytotoxicity, uptake and transformation of nano-CeO_2 in sand cultured romaine lettuce," *Environ. Pollut.* 220, 1400-1408. DOI: 10.1016/j.envpol.2016.10.094

Zhang, M. X., Zhao, L. Y., He, Y. Y., Hu, J. P., Hu, G. W., Zhu, Y., Khan, A., Xiong, Y. C., and Zhang, J. L. (2024). "Potential roles of iron nanomaterials in enhancing growth and nitrogen fixation and modulating rhizomicrobiome in alfalfa (*Medicago sativa* L.)," *Bioresour. Technol.* 391, article ID 129987. DOI: 10.1016/j.biortech.2023.129987

Article submitted: January 25, 2024; Peer review completed: April 30, 2024; Revised version received: April 30, 2024; Accepted: May 3, 2024; Published: May 17, 2024.
DOI: 10.15376/biores.19.3.4434-4454